AC electrokinetics based capture of yeast cells from ultra-fast through-flow for sensitive detection

Quan Yuan[1,2], *Nazmul Islam*[3], *Jie Wu*[1] ✉

[1]*Department of Electrical Engineering and Computer Science, The University of Tennessee, Knoxville, TN 37996, USA*
[2]*Weldon School of Biomedical Engineering, Purdue University, West Lafayette, IN 47906, USA*
[3]*Department of Electrical Engineering, The University of Texas Rio Grande Valley, Edinburg, TX 78539, USA*
✉ *E-mail: jwu10@utk.edu*

Published in Micro & Nano Letters; Received on 10th June 2017; Revised on 18th August 2017; Accepted on 30th August 2017

This work presents a three-dimensional multi-level microfluidic device that enables yeast cell trapping via alternating current (AC) electrokinetics (ACEK) from a rapid through-flow of sample fluids. ACEK is a versatile technique to control and manipulate cells and microparticles at the micro/nano-scale. Here the trapping device works by applying an AC signal over a pair of electrode across a flow-through channel to capture bioparticles from an ultra-fast through-flow. The particle capture effect by ACEK was experimentally studied by measuring the cell densities at the inlet and outlet of the micro-channel. Both symmetric AC signal and DC biased AC signal were used to achieve cell trapping. It is found that DC biased ACEK effect is highly capable of capturing cells from a rapid through-flow. A trapping efficiency of 56.8% has been obtained from an ultra-fast external flow with its average velocity at 4.44 mm/s. The merits of ACEK include low-voltage electrical operation, which is suitable for portable lab-on-a-chip systems. These devices offer numerous benefits for biological applications such as medical diagnostics, detection, drug screening, and particle trapping.

1. Introduction: Yeast cells are responsible for the contamination and spoilage of a variety of food products. Some yeasts develop mycotoxins which diffuse into the product and may, if present in sufficient quantity, cause acute or chronic poisoning. The presence of yeasts leads to changes affecting product quality and scalability, leading to significant financial implications for food producers. It has become imperative to develop a rapid, inexpensive assay that food producers can use to evaluate the level of yeast concentration in the food sample.

However, real-time detection of yeast cells in practical samples could be challenging, especially with the cells present at dilute concentrations. The first step of detection often requires a trapping mechanism of yeast cells from sample solutions to enrich particle counts to a detection level. Microfluidic devices have been developed to extract yeast cells from a flow through system. Many methods have been developed that allow cell manipulation [1–5], including optical, acoustic, magnetic, and electric techniques. For example, Chung *et al.* [4] designed a microfluidic platform for high-density single cell capture by arranging cell traps carefully in a serpentine channel. However, conventional methods to trap yeast cells are cumbersome and unpractical for field-deployable use. Further, to extract sufficient number of cells for detection and analysis, a large volume of sample solution is required, which necessitates the capability to handle rapid through-flow in order to complete the sample processing within a reasonable timeframe.

Here, we developed a simple and portable trapping device to capture yeast cells via alternating current (AC) electrokinetics (ACEK) from rapid through-flow of samples. When applying non-uniform AC electrical fields onto electrolyte through a pair of micro-electrodes, microfluidic phenomena can be induced, which is generally known as ACEK effects. ACEK effects comprise of di-electrophoresis (DEP) on particles, AC electroosmosis (ACEO) and AC electrothermal (ACET) effects on fluid. DEP is manifested as the movement of particles within fluid in response to inhomogeneous applied electric fields, which can be attraction to or repulsion from high electrical field. ACEO and ACET effects induce vortex-like fluidic movements around microelectrodes when AC fields are applied [6–11]. ACEK provides a means to effectively control and manipulate particles and fluids at micro-scale. It is of great interest in recent years because it has important potentials in separating, sorting, and filtering bioparticles, such as cell viruses, bacteria, DNA, and proteins [12–14]. Alternating electric field can be applied exceeding 1 V without causing electrolysis and hence the change of pH value at electrodes, which is inevitable in direct current (DC) electrokinetics. In this work, a parallel plate electrode configuration [15] with a top electrode and a bottom mesh electrode across a micro-channel is adopted to implement the particle trap. An appropriate AC signal applied to the electrode pair induces vortices-like ACET flows around the mesh electrode to extract bioparticles from through-flow for particle enrichment. Here, in order to make the device capable of handling a high through-flow rate, a voltage higher than 1–2 V is needed to induce sufficiently strong ACEK transversal flows [16]. As a 10 V AC signal is used here, operation above a few kHz is required to avoid electrolysis of water, which leaves us the option of using ACET effect. ACET effect can operate at high frequency to avoid electrolysis. Also the AC signal of 10 V at 10 kHz has been reported to be safe to cells as it will not inflict damages to cells [17]. With a second channel below the mesh electrode, the collected particles can be flushed away, or eluted to a separate location for detection, making the device compatible with repeated sampling and downstream analysis. To quantify bioparticle concentration effect, yeast cell concentrations in the through-flow solutions were counted before and after flowing through the trapping electrode. The trapping experiments were conducted at various through-flow rates with two types of electrical signals. The particle trap presented here can be obtained at low cost and is light and small, ready for on-site real-time monitoring [18]. The external components for this trap, such as the pumps and AC signal generators, can also be readily obtained using commercial mini pumps and integrated circuits, thus realising a field deployable system for automated, distributed monitoring of yeast. Further, as yeast cell is a very typical eukaryotic cell and similar to human cell, our device can be used to concentrate most eukaryotic micro-organisms in human as well [19, 20].

2. Mechanism and theory: The device structure is shown schematically in Fig. 1. It consists of four components: (i) channel 1 used to flow sample fluids through the electrical

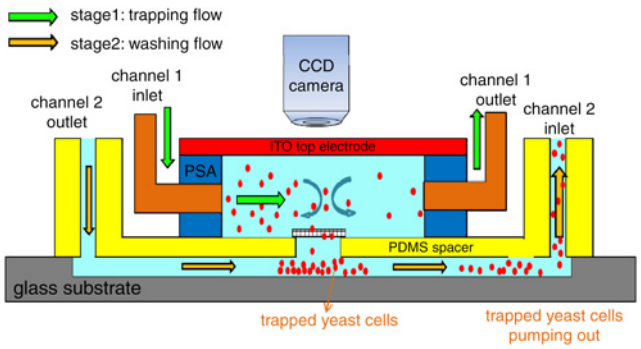

Fig. 1 *Schematic diagram of the 3D multi-level ACEK particle trap for yeast cells capture from a through-flow of sample fluids*

trapping site; (ii) a metallic mesh on the bottom of channel 1, which functions as a trapping electrode and also allows the passage of particles from channel 1 to channel 2; (iii) a counter electrode embedded in the top of channel 1 faces the mesh electrode; (iv) channel 2, into which the particles are collected and later on eluted or flushed away.

As shown in Fig. 1, an AC signal applied between the mesh and top electrodes will induce ACET effects and produce transversal flows across the through-flow streamlines in channel 1. Due to three-dimensional (3D) micro-topology of the mesh electrode, electrical fields around it are non-uniform. As a result, ACET microflows are generated above and around the mesh electrode, which acted as the major factor to bring particles from channel 1 through the mesh electrode into channel 2. Gravity also plays a part in sending the cells down through the mesh electrodes. The frequency and voltage are chosen such that the device operates at a frequency inducing weak to negative DEP, to ensure contact-free and reusable trapping.

2.1. ACET effect: Theoretically, ACET mechanism involves the coupling between electric, thermal, and fluidic dynamics formulations. ACET flows arise from the interaction between electrical fields and gradients of conductivity and permittivity which can be generated by temperature gradient. When an AC signal is applied to electrodes in an electrolyte, an electric field is established within the electrolyte with electrical conductivity, σ, Joule heating of the fluid will take place according to the energy balance equation [21, 22]

$$k\nabla^2 T + \frac{1}{2}\langle \sigma E^2 \rangle = 0 \tag{1}$$

where k is the thermal conductivity, T is the temperature, and σ is the electric conductivity of the fluid. σE^2 represents the power density generated in the fluid by Joule heating from the applied electric fields.

For our micro-channel, heat convection is small compared with heat diffusion. So the energy balance equation here assumes the simplified form with Joule heating as the energy source. If the field strength E is non-uniform, there will be spatial variation in heat generation, which leads to temperature gradient ∇T in the fluid. In turn, the temperature gradient produces spatial gradient in fluid conductivity and permittivity given by $\nabla\varepsilon = (\partial\varepsilon/\partial T)\nabla T$ and $\nabla\sigma = (\partial\sigma/\partial T)\nabla T$. $\nabla\varepsilon$ and $\nabla\sigma$ induce mobile charges ρ_e in the bulk fluid according to $(\partial\rho_e/\partial t) + \nabla\cdot(\sigma E) = 0$ and $\rho_e = \nabla\cdot(\varepsilon E)$. These free charges move under electric field and drag the fluid through viscosity $F_{et} = \rho_e E - (1/2)|E|^2\nabla\varepsilon$.

The time averaged ACET force density on fluid is then

$$F_{et} = -0.5\left[\left(\frac{\nabla\sigma}{\sigma} - \frac{\nabla\varepsilon}{\varepsilon}\right)E_0\frac{\varepsilon E_0}{1+(\omega\tau)^2} + 0.5|E_0|^2\nabla\varepsilon\right] \tag{2}$$

where σ and ε are the electrical conductivity and permittivity of the medium, $\tau = \varepsilon/\sigma$ is called charge relaxation time, and $\omega = 2\pi f$ is radian frequency. E_0 is the magnitude of the applied electric field. Obviously, the magnitude of ACET force relies on the strength of electrical field and temperature gradient since σ and ε are dependent on temperature. From (2), it can be deduced that the fluid body force F_{et} follows the direction of electric field and is proportional to the temperature gradient ∇T. The fluid behaviour is governed by Navier–Stokes equation $\rho(\partial u/\partial t) + \rho(\nabla\cdot u)u - \eta\nabla^2 u + \nabla P = F_{et}$, where ρ is the fluid density, η is the dynamic viscosity, P is the external pressure, and u is the velocity of the fluid. Together with $\nabla\cdot u = 0$ for incompressible fluid, fluid velocity can be determined for ACET flow.

The temperature gradients increase linearly with conductivity and so ACET flow is especially suitable for manipulation of conductive solutions. ACET effect is also suitable for medium to high frequency (10 kHz for our experimentation) operation, which will minimise electrode corrosion when subjected to electric field in an electrolyte. The ACET velocity depends on the applied voltage greatly, with the ACET velocity u increasing with the applied voltage $V_{\rm rms}$ as $u \propto V_{\rm rms}^4$. So ACET flow can become considerably stronger with only moderate increase of applied voltage [23].

In this work, the face-to-face configuration of an electrode pair was used to generate ACET microflows (Fig. 1). The lower electrode was made of woven metal wires with periodical openings, which generates non-uniformity in electrical field distribution. This type of electrodes has been shown to induce microflows around the electrodes by both ACEO and ACET effects [24, 25]. Fig. 2 shows COMSOL simulation of fluid velocity distribution around a set of wire electrodes (representing the cross-sectional view of a mesh electrode). A through-flow with an average linear velocity of 1000 µm/s was applied to the inlet (left side), the outlet of channel 1 and channel 2 (right side) was set as open boundary in dynamic fluidic field simulation. A 5 V amplitude AC signal at 10 kHz was applied between the top indium-tin-oxide (ITO) glass and the mesh electrodes in this case. The mesh electrode and the inlet of channel 1 were set at a constant temperature of 300 K for thermal field simulation, since the temperature of fresh yeast cell solution and mesh electrodes with high thermal conductivity are close to room temperature. The simulated flow field plot has combined the effects of ACET, DEP, and gravity on the cells. As can be seen from Fig. 2, fluid motions are generated by applying AC electric signal between mesh electrodes and ITO glass slide. Vortices are formed around the wire electrodes. With combined effects from ACET flow, DEP force, and gravity, yeast cells will

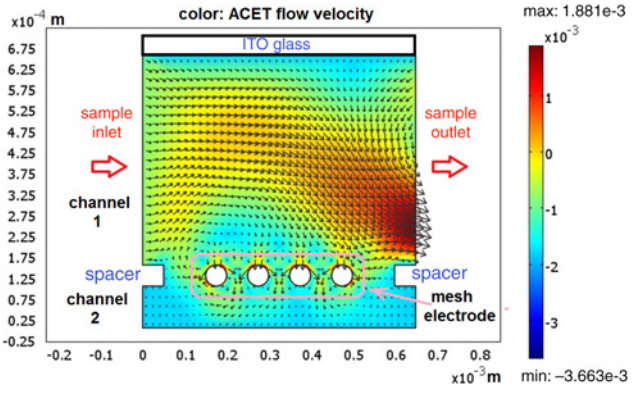

Fig. 2 *COMSOL simulation of flows that yeast cells experience around a set of wire electrodes in the trapping channel. An external through-flow with an average linear velocity of 1000 µm/s was applied from the left inlet to channel 1. The cells also experience ACET flows, negative DEP force, and gravity. The colour legend represents the magnitude of micro-flow field, and the arrows show the flow directions*

doi: 10.1049/mnl.2017.0424

undergo strong downwards movements between the wires, which bring them down towards the bottom channel. Once the cells fall into the space below the wire electrodes, there is no electrical field and also very weak upwards return flows. Therefore, the cells will become trapped.

2.2. DC biased ACET effect: Adding a DC term with an AC signal will lead to higher ACEK velocity, although with different mechanisms for ACEO [26] and ACET effects [27]. Biased ACET effect is implemented by energising the bottom electrode with a positive DC voltage superimposed onto the AC signal between the top and bottom electrodes. A DC bias will produce coions near the electrodes due to Faradaic reactions. As the time averaged force exerted by an AC field on a free ion is zero, those ions do not contribute to ACET flows directly. Nevertheless, the generated ions may increase the local ionic strength near the electrodes and could lead to substantial $\nabla\sigma/\sigma$, which will induce strong ACET microflows according to (2), hence producing powerful vortices across the through-flow streamlines for particle collection.

Further, yeast cells have negative surface charges in pH neutral aqueous environment. By adding a DC bias with the positive potential at the mesh electrode, the cells will experience electrophoresis force towards bottom electrode (positive charge) as well.

2.3. Dielectrophoresis: DEP refers to the force exerted on an uncharged particle in aqueous medium induced by non-uniform electric fields [28]. The effectiveness of this method depends on how polarised the particles are with respect to the fluid medium. The magnitude of DEP force is expressed as

$$\langle F_{\mathrm{DEP}}\rangle = \pi\varepsilon_{\mathrm{m}}a^3\mathrm{Re}\left[\frac{\tilde{\varepsilon}_{\mathrm{p}}-\tilde{\varepsilon}_{\mathrm{m}}}{\tilde{\varepsilon}_{\mathrm{p}}+2\tilde{\varepsilon}_{\mathrm{m}}}\right]\nabla|E^2|o \tag{3}$$

where a is the particle diameter, ε_{p} is the particle permittivity, and ε_{m} is the permittivity of the suspending medium. The magnitude of the force also depends on the permittivity of the suspending medium. In the case of E denoted by a point charge

$$E\propto\frac{1}{r},\quad \nabla|E^2|\propto\frac{1}{r^3} \tag{4}$$

DEP force can be attractive or repulsive, depending on the sign of the term $[(\tilde{\varepsilon}_{\mathrm{p}}-\tilde{\varepsilon}_{\mathrm{m}})/(\tilde{\varepsilon}_{\mathrm{p}}+2\tilde{\varepsilon}_{\mathrm{m}})]$ in (3). Positive DEP (pDEP) attracts particles to high electrical field regions, while negative DEP (nDEP) repels particles from high field regions and directs the particle to low field regions. The AC signal used for ACET also induces nDEP to avoid bioparticle adhesion to the electrodes. In this work, as the first step, the dielectropheretic property of model yeast in water was characterised to evaluate the feasibility of trapping yeast by the combined effects of ACET and nDEP. Therefore, a frequency range that is suitable for inducing both ACET and nDEP was applied.

3. Experiments

3.1. Fabrication: A low-cost desktop fabrication method was used to prototype this 3D multi-level concentrator [29]. The device structure is shown schematically in Fig. 3. One glass slide was used as the base of the device. The channels were made of pressure sensitive adhesive (PSA) tape and cut into desired geometries by a digital craft cutter (Quickutz Silhouette SD).

In the first phase of fabrication, we attached a layer of PSA tape on the cleaned glass slide uniformly (remove all air bubbles). Then we cut the attached PSA tape into channel 2 with openings for the inlet and outlet. The dimensions of channel 2 are 50 mm × 2 mm × 100 µm ($L\times W\times H$). Two pre-fabricated Polydimethylsiloxane (PDMS) tubes were attached as the inlet

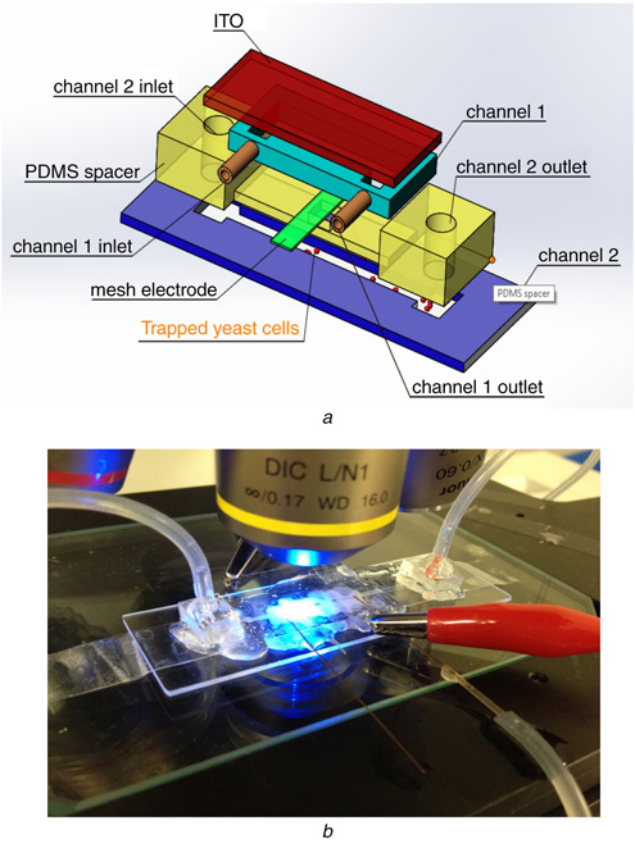

Fig. 3 *Schematic illustration and experimental set-up of the trapping device*
a Schematic illustration of 3D multi-level microfluidic device for yeast cell trapping
b Experimental set-up under a Nikon microscope with electrical connections and the connections to an external flow-through pumping system

and outlet. After that, a stripe of metal mesh electrode was placed across the top of channel 2. The mesh electrode was woven from 20 µm diameter wires with openings of 45 µm × 45 µm. This electrode was made by cutting a strip from a metal filter (06457-AB) manufactured by SPECTRUMLABS. The mesh electrode was cut to be 1 mm wide, forming a trapping area of 1 mm × 1.5 mm in channel 1. Channel 1 was fabricated with the same procedure with PSA as that for channel 2 with a cross-sectional area of 1.5 mm (W) × 1 mm (H). In our device, two electrodes with different sizes are face-to-face embedded into channel 1. The larger electrode on top of channel 1 was built by an ITO slide, which is a transparent conductor for observation and also as the top cover of channel 1. Epoxy glue is used to seal any leaks in the device. It takes around 4 h (include 3 h PDMS curing time) to fabricate a 3D multi-level microfluidic pre-concentrator. A photograph of the bioparticle concentrator is shown in Fig. 3*b*. The sample solution will be pumped through the top channel 1 and the embedded particles will be trapped through the mesh electrode into channel 2.

3.2. Microfluidic experiments: In the preliminary tests, yeast cells were used as the model particle in water with an electrical conductivity of 0.02 S/m. For trapping experiments, the sampling and flushing flows through the particle trap were produced by two external syringe pumps (NE-1000 programmable single syringe pump, Pump systems Inc), one for each channel. Channel 1 was primed with sampling fluid with yeast suspension for trapping, and channel 2 was prefilled with purified freshwater buffer. During the trapping experiments, the pump for channel 2 was shut off, and the pump for channel 1 stayed on to provide the sampling flow. The syringe pump for channel 1 was put on

a shaker during injection to keep yeast suspended in the fluid throughout the experiment. Hemocytometers were used to measure the concentration level for each sample.

The AC trapping signal was generated by a 50 MHz function/pulse signal generator 8551 (Tabor Electronics Ltd, USA). An oscilloscope MSO6012A (Agilent technology, USA) was used to monitor the actual voltage drop over the electrode in real time. The applied AC signal on the electrodes was 8–10 V in amplitude at 10 kHz. The trapping process was observed through a microscope (Nikon, LV100). Image processing software 'Image-Pro 3D suite' was used for subsequent data analysis. The greyscale of a clean device prior to trapping was used as the background control. Image-Pro 3DS software was also used for particle image velocimetry analysis to characterise micro-flow velocities.

4. Results and discussion: As discussed earlier, nDEP were used for trapping of yeast cells. DEP effect is frequency dependent, and DEP can change between pDEP (attraction) and nDEP (repulsion) with frequency. ACET flows usually occur in the mid/high frequency range. First of all, DEP characteristics for yeast cells in water were studied. A single pair of interdigitated gold electrodes was used for that purpose. Obvious ACET flow was observed with 10 V in amplitude at 10 kHz. Our experiments showed that high fluid velocity was produced by the applied voltage. nDEP of yeast cells was observed at frequencies below 10 kHz and coexisted with the ACET effect. The particles were repelled from the electrodes, and strong fluid motion was formed and circulated continuously at the surface of the electrodes. Positive DEP phenomenon was observed with an AC signal of 5 MHz and 6 V. Therefore, the AC frequency for our device was chosen to be 10 kHz.

Proof of concept experiments was conducted using yeast cells for test. Particle trapping was demonstrated at low voltage no more than 10 V in amplitude at 10 kHz. The whole trapping procedures are demonstrated under microscope (Nikon, LV100). Figs. 4*a–d* show the result of particle trapping when the AC signal has been applied to the electrode for 60, 120, 180, and 210 s, respectively. The increase in particle concentration at the centre of the grid can be easily seen. Fig. 4*e* shows the electrode mesh grid after the wash. Nearly all the particles are gone. This proves that the ACEK trap can effectively trap and release particles.

Next, the particle concentration effects were quantitatively characterised by measuring the cells densities at the inlet and outlet of channel 1. The trapping experiments under each condition were repeated and measured three times. The difference in the cell concentration before and after passing the trapping channel indicates the extent of cells being held within the trapping channel. Since the cells are also subject to sedimentation effect that will lead to cell deposition in the channel, control experiments were also run in which no AC signal is applied. The control experiments quantify the loss of cells due to sedimentation when flowing through the channel. Marienfeld counting chambers were used in the experiments.

The trapping efficiency of yeast cells depends on the flow rate of external through-flow. As flow rate increases, the travelling velocity of yeast cells increases too. A faster through-flow will bring in more yeast cells for trapping. However, too fast a flow velocity will make trapping more difficult, because the time for yeast cells passing through the trapping electrode becomes shorter and hence less time for ACET effect to act on the yeast cells. There is, therefore, a trade-off for an optimised flow velocity to extract yeast cells from high throughput enrichment. Consequently, several different

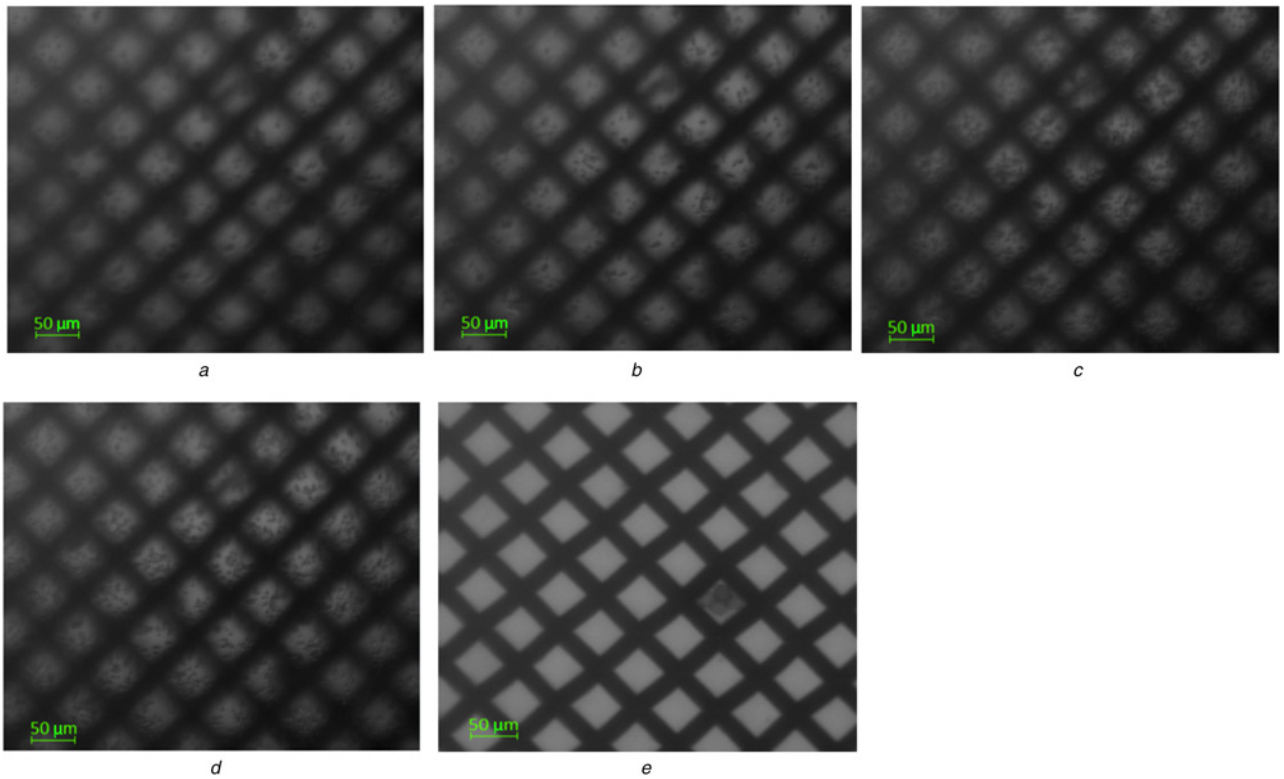

Fig. 4 *Yeast cell trapping process observed under a Nikon microscope. Time-lapse photographs of yeast cells trapped below a mesh electrode following power on*
a 60 s
b 120 s
c 180 s
d 210 s
e Clean mesh electrode after wash

doi: 10.1049/mnl.2017.0424

external flow rates (0.1, 0.2, 0.3, 0.4, 0.5 ml/min) have been used in the experiment to find the trapping efficiency under various flow-through velocities.

In the first set of trapping experiments, symmetric AC signal of 10 V in amplitude at 10 kHz was used. The cell concentrations at the inlet of channel 1 were maintained to be around 960 cells/µl for all experiments, labelled as 'original' in Fig. 5. The cell concentrations at the outlet are given in two groups, a control group without any AC signal with the data columns in green, a group with AC signal on with the data columns in red. The green control group captures the effects from cell sedimentation and hydrodynamic drags over a mesh electrode, while the red ACEK active group represents the situations when an AC signal is turned on to trap cells with additional effects possibly from ACET and DEP forces. By comparing the ACEK active and control groups, the effects of applied AC signal are illustrated. The difference between the control and ACEK active groups represents the amount of cells trapping by ACEK effects.

Fig. 5 gives yeast cell concentrations at the channel 1 outlet for various external flow velocities. For every flow rate, there are two columns showing the particle densities. The left columns are the results from control experiments, in which no AC signal was applied, and the right columns are results with an AC signal applied between the top ITO glass and the mesh electrode.

In Fig. 5, it can be seen that as through-flow velocity decreases, the cell concentration at the outlet goes down accordingly for both the control and ACEK active groups. For the control group, the differences between the 'original' column and green columns account for particles lost in the channel due to sedimentation. The decrease in the magnitude of control columns with decreasing flow rate is due to more sedimentation time for cells as they flow through channel 1. For the ACEK active group, the ACEK trapping is also more pronounced at lower flow rates, because there is longer time for induced ACET flows to carry particles to the mesh electrodes in addition to the effect of sedimentation. At any flow rate, the ACEK active cases will yield lower cell concentrations than their corresponding controls, demonstrating the trapping effect from an AC signal. However, the lowest flow rate does not necessarily lead to the highest trapping efficiency, i.e. the portion of cells being trapped due to ACEK effects. The trapping efficiency for different external flow rate has been calculated and given in Table 1. Here, the trapping efficiency is defined as $(C_{np}-C_p)/C_{np}$, where C_{np} is the yeast concentration at the channel 1 outlet without applying a voltage [i.e. the control group (green columns)], and C_p is the yeast concentration at the channel 1 outlet with the AC signal on (i.e. the red columns).

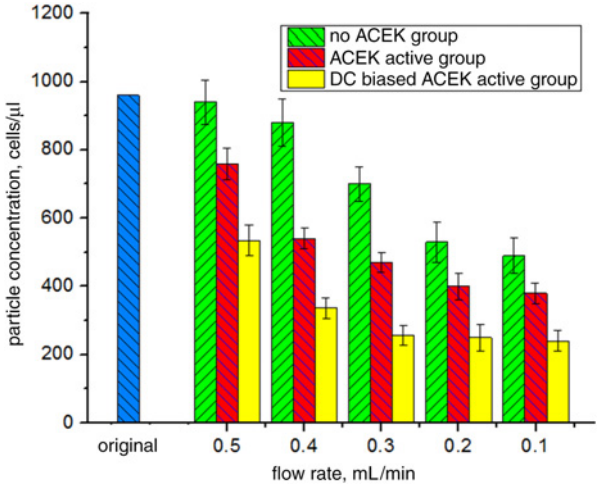

Fig. 5 *Yeast concentrations at the channel 1 outlet at various external flow rates. Two types of trapping signals were used, symmetric AC and AC with a DC bias. Green (right-slanted) columns are results when no AC voltage was applied, while red (left-slanted) columns are results with a symmetric AC signal applied, and yellow (no pattern) columns are results when using a DC biased AC signal*

The trapping efficiency is given in terms of percentage in Table 1. As expected, the lowest trapping efficiency of 19.15% happens at a high flow rate of 0.5 ml/min, corresponding to an average linear fluid velocity of 5.55 mm/s. It is probably because the external flow becomes too strong for ACET flows to carry cells to the mesh electrode. However, the trapping efficiency at low flow rate is also low, 22.46–24.31% for a flow rate of 0.1–0.2 ml/min, while the lowest amount of cells can go through channel 1 and appear at its outlet at this range of flow rates. In contrast, the highest trapping efficiency is 38.63%, present at 0.4 ml/min. The reason could be that a significant portion of cells are lost to sedimentation and fewer cells are available to be trapped, which leads to lower trapping efficiency at lower flow rate. This explanation is supported by the fact that cell concentration at the outlet is obviously reduced when the flow rate becomes lower than 0.4 ml/min.

The second set of experiments was conducted using a DC biased AC signal. Based on our prior work, ACET flow velocity can be greatly enhanced by adding a DC bias. The hypothesis is that a higher trapping efficiency can be obtained by increasing ACET velocity. The applied signal is 1 V_{dc} with an AC signal of 8 V in amplitude at 10 kHz. All other parameters remained identical to those of the previous experiments.

The trapping results using biased ACET effect are shown in Fig. 5 as the un-patterned columns. The change in cell concentration at the outlet shows a similar trend with decreasing flow rate to that of ACEK active group. What is different from the symmetric ACEK group is that the cell concentrations at the outlet were much lower with DC biased ACEK trapping. Again, the trapping efficiencies at various flow rates were calculated and presented in the last row of Table 1. From Fig. 5 and Table 1, it can be conclude that trapping efficiency has improved when using DC biased ACET effect. A trapping efficiency of 56.3% was achieved at an average linear fluid velocity of 4.44 mm/s, increasing from 38.6% when using a symmetric AC signal. At 5.55 mm/s, the trapping efficiency has increased from 19.2% when using a symmetric AC signal to 41.7% when using a DC biased AC signal. However, at 0.1 ml/min (1.11 mm/s), there is no significant increase in trapping efficiency with its being 22.5 and 25.2%, respectively, suggesting that the trapping is possibly limited by the supply of cells.

Further, the trapping efficiency with different initial cell concentrations has been tested and given in Table 2. AC signal of 10 V in amplitude at 10 kHz with external pumping flow rates 0.4 ml/min has been provided during the experiment with four initial

Table 1 Trapping efficiency using symmetric AC signal and DC biased AC signal with different external flow rates

flow rate, ml/min	0.5	0.4	0.3	0.2	0.1
average velocity, mm/s	5.55	4.44	3.33	2.22	1.11
		symmetric ACEK trapping			
trapping efficiency, %	19.2	38.6	32.8	24.3	22.5
		DC biased ACEK trapping			
trapping efficiency, %	41.7	56.8	43.6	34.8	25.2

Table 2 Trapping efficiency for different initial cell concentrations

initial cell concentration, cells/μl	960	720	480	240
trapping efficiency, %	38.6	38.7	37.1	36.2

concentrations 240, 480, 720, and 960 cells/μl. The trapping efficiency has not changed greatly and only a slightly decreasing was observed, which means our device is applicable for a broad range of cells with different concentrations.

The impedance at 10 kHz about our device is around 3.8 kΩ and the current generated via AC signal in solution is <300 μA which is too small to damage the cells. The trapped cells demonstrate similar biological growth rates with the initial cells, and this is another proof that the trapped cells are not damaged by the applied AC signal.

5. Conclusion: This Letter described a novel particle trapping microfluidic device based on DC biased ACET technology. We have successfully demonstrated extraction of yeast cells from a rapid flow-through sample solution for high throughput. By using the DC biased ACET flow, we can also improve the trapping efficiency up to 56.8% from an ultra-fast external through-flow with a fluid velocity of 4.4 mm/s. The merits of our device include high throughput, good trapping efficiency, low cost, simple operation, portability, and reusability. Further system miniaturisation and integration can be readily achieved by incorporating mini pump and IC control. For example, using mini Pumps from Takasago Fluidic Systems, AD9834, microcontroller and other peripherals such as an antenna, the particle trapping system can be readily made portable. The overall power consumption for the entire device can be controlled to within 300 mW, which makes the device feasible to use with battery.

6. Acknowledgments: This research was supported by funding from Oak Ridge National Laboratory's (ORNL) Technology Transfer and Economic Development Maturation funding program, and the University of Tennessee Initiative for PON/POC Nanobiosensing.

7 References

[1] Weibel D.B., Diluzio W.R., Whitesides G.M.: 'Microfabrication meets microbiology', *Nat. Rev. Microbiol.*, 2007, **5**, pp. 209–218
[2] Lindstrom S., Andersson-Svahn H.: 'Overview of single-cell analyses: microdevices and applications', *Lab Chip*, 2010, **10**, pp. 3363–3372
[3] Nilsson J., Evander M., Hammarstrom B., *ET AL.*: 'Review of cell and particle trapping in microfluidic systems', *Anal. Chim. Acta*, 2009, **649**, pp. 141–157
[4] Chung K., Rivet C.A., Kemp M.L., *ET AL.*: 'Imaging single-cell signaling dynamics with a deterministic high-density single-cell trap array', *Anal. Chem.*, 2011, **83**, pp. 7044–7052
[5] Wu J.: 'Biased AC electroosmosis for on-chip bioparticle processing', *IEEE Trans. Nanotech.*, 2006, **5**, (2), pp. 84–89
[6] Wu J.: 'Interactions of electrical fields with fluids: laboratory-on-a-chip applications', *IET Nanobiotechnol.*, 2008, **2**, pp. 14–27
[7] Ramos A., Morgan H., Green N.G., *ET AL.*: 'AC electric-field-induced fluid flow in microelectrodes', *J. Colloid Interface Sci.*, 1999, **217**, pp. 420–422
[8] Bazant M.J.: 'AC electro-osmotic flow', in Dongqing Li (Ed.): 'Encyclopedia of microfluidics and nanofluidics' (Springer, New York), 2008, pp. 8–14
[9] Wu J., Ben Y., Battigelli D., *ET AL.*: 'Long-range AC electroosmotic trapping and detection of bioparticles', *Ind. Eng. Chem. Fundam.*, 2005, **44**, pp. 2815–2822
[10] Islam N., Lian M., Wu J.: 'Enhancing cantilever capability with integrated AC electrokinetic trapping mechanism', *J. Microfluid. Nanofluid.*, 2007, **3**, pp. 369–375
[11] Yuan Q., Yang K., Wu J.: 'Optimization of planar interdigitated microelectrode array for biofluid transport by AC electrothermal effect', *Microfluid. Nanofluid.*, 2014, **16**, pp. 167–178
[12] Studer V., Pépin A., Chen Y., *ET AL.*: 'An integrated AC electrokinetic pump in a microfluidic loop for fast and tunable flow control', *Analyst*, 2004, **129**, pp. 944–949
[13] Ivanoff C.S., Wu J., Mirzajani H., *ET AL.*: 'AC electrokinetic drug delivery in dentistry using an interdigitated electrode assembly powered by inductive coupling', *Biomed. Microdevices*, 2016, **18**, p. 84
[14] Cui H., Cheng C., Lin X., *ET AL.*: 'Rapid and sensitive detection of small biomolecule by capacitive sensing and low field AC electrothermal effect', *Sens. Actuators B*, 2016, **226**, pp. 245–253
[15] Wu J., Islam N.: 'A simple method to integrate in-situ nano-particle focusing with cantilever detection', *IEEE Sens. J.*, 2007, **7**, pp. 957–958
[16] Yang K., Wu J.: 'Numerical study of in situ preconcentration for rapid and sensitive nanoparticle detection', *Biomicrofluidics*, 2010, **4**, (3), p. 034106
[17] Kirson E.D., Dbalý V., Tovaryš F., *ET AL.*: 'Alternating electric fields arrest cell proliferation in animal tumor models and human brain tumors', *PNAS*, 2007, **104**, (24), pp. 10152–10157, doi:10.1073/pnas.0702916104
[18] Kordialik-Bogacka E.: 'Surface properties of yeast cells during heavy metal biosorption', *Cent. Eur. J. Chem.*, 2011, **9**, (2), pp. 348–351
[19] Asami K., Hanai T., Koizumi N.: 'Dielectric properties of yeast cells', *J. Membrane Biol.*, 1976, **28**, pp. 169–180
[20] Lew D.J., Dulic V., Reed S.I.: 'Isolation of three novel human cyclins by rescue of G1 cyclin (cln) function in yeast', *Cell*, 1991, **66**, pp. 1197–1206
[21] Lian M., Wu J.: 'Microfluidic flow reversal at low frequency by AC electrothermal effect', *Microfluid. Nanofluid.*, 2009, **7**, (6), pp. 757–765
[22] Wu J., Lian M., Yang K.: 'Micropumping of biofluids by AC electrothermal effects', *Appl. Phys. Lett.*, 2007, **90**, p. 234103
[23] Gonzalez A., Ramos A., Morgan H., *ET AL.*: 'Electrothermal flows generated by alternating and rotating electric fields in microsystems', *J. Fluid Mech.*, 2006, **564**, pp. 415–433
[24] Lian M., Islam N., Wu J.: 'AC electrothermal manipulation of conductive fluids and particles for lab-chip applications', *IET Nanobiotechnol.*, 2007, **1**, (3), pp. 36–43
[25] Wu J., Islam N., Lian M.: 'High sensitivity particle detection by biased AC electro-osmotic trapping on cantilever'. 19th IEEE Int. Conf. on Micro Electro Mechanical System (MEMS), 22–26 January 2006, pp. 566–569
[26] Wu J.: 'AC electroosmotic micropump by asymmetric electrode polarization', *J. Appl. Phys.*, 2008, **103**, p. 024907
[27] Lian M., Wu J.: 'Ultra fast micropumping by biased AC electrokinetics', *Appl. Phys. Lett.*, 2009, **94**, p. 064101
[28] Pethig R.: 'Review article-dielectrophoresis: status of the theory, technology, and applications', *Biomicrofluidics*, 2010, **4**, (2), p. 022811
[29] Yuan Q., Wu J., Greenbaum E., *ET AL.*: 'A resettable in-line particle concentrator using AC electrokinetics for distributed monitoring of microalgae in source waters', *Sens. Actuators B*, 2017, **244**, pp. 265–274

doi: 10.1049/mnl.2017.0424